



Nonlinear Mixed-Effects (NLME) Diameter Growth Models for Individual China-Fir (*Cunninghamia lanceolata*) Trees in Southeast China

Hao Xu¹, Yujun Sun^{1*}, Xinjie Wang¹, Yao Fu¹, Yunfei Dong¹, Ying Li²

¹ The Key Laboratory for Silviculture and Conservation of Ministry of Education, College of Forestry, Beijing Forestry University, Beijing, PR China, ² College of Forestry, Beijing Forestry University, Beijing, PR China

Abstract

An individual-tree diameter growth model was developed for *Cunninghamia lanceolata* in Fujian province, southeast China. Data were obtained from 72 plantation-grown China-fir trees in 24 single-species plots. Ordinary non-linear least squares regression was used to choose the best base model from among 5 theoretical growth equations; selection criteria were the smallest absolute mean residual and root mean square error and the largest adjusted coefficient of determination. To account for autocorrelation in the repeated-measures data, we developed one-level and nested two-level nonlinear mixed-effects (NLME) models, constructed on the selected base model; the NLME models incorporated random effects of the tree and plot. The best random-effects combinations for the NLME models were identified by Akaike's information criterion, Bayesian information criterion and -2 logarithm likelihood. Heteroscedasticity was reduced with two residual variance functions, a power function and an exponential function. The autocorrelation was addressed with three residual autocorrelation structures: a first-order autoregressive structure [AR(1)], a combination of first-order autoregressive and moving average structures [ARMA(1,1)] and a compound symmetry structure (CS). The one-level (tree) NLME model performed best. Independent validation data were used to test the performance of the models and to demonstrate the advantage of calibrating the NLME models.

Citation: Xu H, Sun Y, Wang X, Fu Y, Dong Y, et al. (2014) Nonlinear Mixed-Effects (NLME) Diameter Growth Models for Individual China-Fir (*Cunninghamia lanceolata*) Trees in Southeast China. PLoS ONE 9(8): e104012. doi:10.1371/journal.pone.0104012

Editor: Rongling Wu, Pennsylvania State University, United States of America

Received: February 18, 2014; **Accepted:** July 6, 2014; **Published:** August 1, 2014

Copyright: © 2014 Xu et al. This is an open-access article distributed under the terms of the Creative Commons Attribution License, which permits unrestricted use, distribution, and reproduction in any medium, provided the original author and source are credited.

Funding: Total expense of field investigation was borne by the Special Public Interest Research and Industry Fund of Forestry (No. 200904003-1) and the project of forestry science and technology research (No. 2012-07). The funders had no role in study design, data collection and analysis, decision to publish, or preparation of the manuscript.

Competing Interests: The authors have declared that no competing interests exist.

* Email: sunyj@bjfu.edu.cn

Introduction

China-fir (*Cunninghamia lanceolata* (Lamb.) Hook) is the most commonly grown afforestation species in southeast China because of its fast growth and good wood qualities. It is widely used for buildings, furniture, bridge construction and many other purposes.

Growth and yield models are commonly used for forest management planning because they can simulate stand development and production under various management alternatives [1,2]. Individual-tree diameter growth models are a fundamental component of forest growth and yield prediction frameworks [3–5]. The models are based on extensive growth data obtained from diverse regions and management levels. Individual-tree diameter growth can be expressed as a function of tree size, competitive effect, stand structure and site quality [6]. A distance-independent individual-tree model structure may be flexible enough to predict diameter growth in monospecific even-aged stands and in mixed-species and multi-aged stands [7].

Regression analysis, such as ordinary non-linear least squares (ONLS) regression, is the most commonly used statistical method in forest modeling [8]. Individual-tree diameter growth models have been fitted to growth increment data collected repeatedly over time on the same tree [9]. The hierarchical nature of the data results in spatial and temporal correlation among observations

made in the same sampling unit (i.e., plot and tree) [10]. However, the stochastic structure is often ignored and independence of observations is assumed [11–15]. Furthermore, the data are autocorrelated and cannot be considered independent samples of the basic tree population [10]. The ONLS regression assumption of independent residuals is therefore violated, biasing the estimates of the standard error of the parameter estimates [16]. Many recent efforts to develop diameter growth models have used nonlinear mixed-effects (NLME) models [5,17].

NLME models include both fixed effects, which are parameters associated with an entire population or with certain repeatable levels of experimental factors, and random effects, which are associated with individual experimental units drawn at random from a population [18]. Random effects account for spatial and temporal correlation by defining the covariance structure of the model's random components and by using this structure during parameter estimation. NLME models provide an efficient statistical method for explicitly modeling hierarchical stochastic structure. Growth models can be calibrated by predicting random components from tree- or plot-level covariates when a new subject is available and is not used in the fitting of the model by using the empirical best linear unbiased predictors (EBLUPs) [3,4,12,19].

Statistical models in which both fixed and random effects enter nonlinearly are increasingly common in the biosciences [20]. The

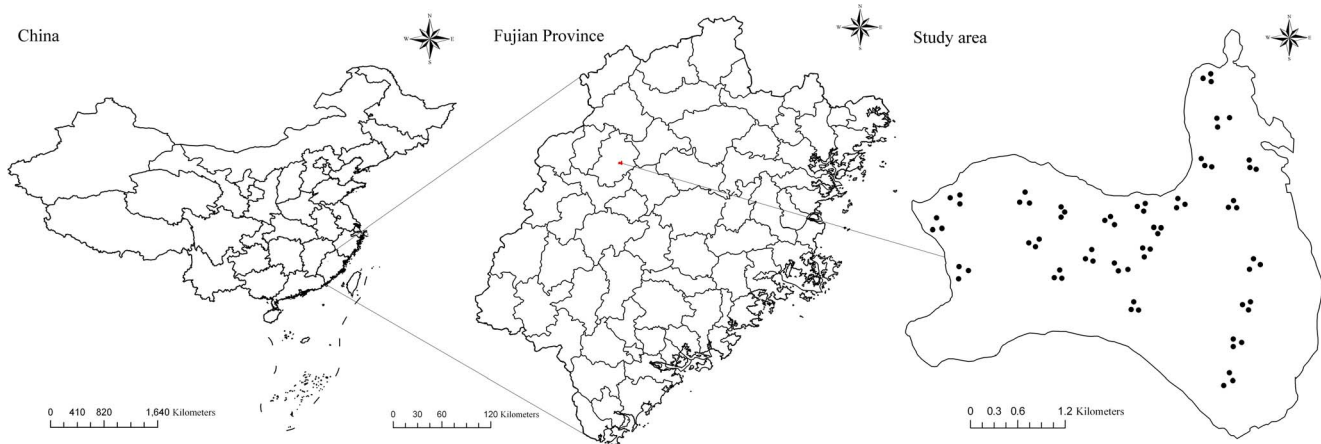


Figure 1. Seventy two trees in twenty four sample plots on Jiangle state-owned forest farm in southeast China.
doi:10.1371/journal.pone.0104012.g001

models are relevant to many disciplines, including forestry, agriculture, ecology, biology, biomedicine and pharmacokinetics [21]. They are used to analyze data with complex structures, including grouped data, longitudinal data, repeated measures data and multivariate multilevel data [22]. One of the most common applications is for analysis of nonlinear growth data [23]; these are data measured repeatedly over time on the same tree (multiple observations obtained from the same sampling unit or subject in sequence over time) and are also known as longitudinal data [12,24].

The main purpose of this study was to develop an individual-tree diameter growth model for *C. lanceolata* (Lamb.) Hook growing in Fujian province, southeast China. The data were derived from 144 increment cores from 72 trees in 24 sample plots. One-level and nested two-level nonlinear mixed modeling approaches that included both fixed and random components were applied to the hierarchical structure of the data. This diminished the level of variance among the sampling units, which were included as covariates. In developing the diameter growth models, we considered nested two-level models and a single-level model. The first level is the plot and the second level is the tree, nested within the plot. Our preliminary analysis showed that the NLME models with random effects effectively removed the heteroscedasticity and autocorrelations in the repeated-measure data and therefore could be important tools for sustainable management of China-fir species within the study area. The predictive ability of the developed model and the applicability of the NLME model were demonstrated using separate validation data.

Materials and Methods

Data

The data were obtained from 24 single-species plots of plantation-grown China-fir on the Jiangle state-owned forest farm in southeast China (Figure 1). One-hundred and forty-four increment cores were collected from 72 trees; 15 cores missed the pith and were excluded from analysis. The increment cores were extracted from three mean trees in each plot; the mean trees were trees with a diameter at breast height (dbh; 1.3 m above ground) approximately equal to the plot mean dbh. Two cores were collected perpendicular to each other from each tree at breast height. The sample plots were square and varied in size from 400 to 600 m². All standing live trees (height >1.3 m) on the plots

were measured for dbh (outside bark) and tree height. Three to five dominant trees on each plot were chosen to calculate plot dominant height. Using the Lintab tree-ring measurement system (Rinntech Company in Germany), the width of each annual growth ring (radial increment data) was measured; trees were assumed to be round, so the diameters were calculated as twice the radius. Growth data from the seed orchard at the forest farm indicate that China-fir requires two years to attain a height of 1.3 m. Diameter data were therefore assigned an initial age of 3 years. Independent data were used for model validation. The data were randomly divided into two groups; 75% of the points were used for model fitting, and 25% were used for model validation. The fitting data and the validation data included 54 trees from 23 plots and 18 trees from 13 plots, respectively. Summary statistics for both fitting and validation data are shown in Table 1.

Methods

Nested two-level NLME model. The model data were derived from the measured annual increment of the sampled trees. The nested sampling structure created a high degree of correlation among observations taken from the same tree and plot. The mixed-effects modeling approach is a common means of addressing the correlation structure in the data [13,23]. A general expression for a NLME model can be defined as [22,25].

$$DBH_{ijk} = f(\phi_{ij}, t_{ijk}) + \varepsilon_{ijk}, \quad i = 1, \dots, M, \quad j = 1, \dots, M_i, \quad k = 1, \dots, n_{ij} \quad (1a)$$

where M is the number of plots, M_i is the number of trees within the i th plot, and n_{ij} is the number of observations (increments). DBH_{ijk} is the dbh (cm) at the k th age of the j th tree taken from the i th plot, t_{ijk} is the age, ϕ_{ij} is the parameter vector $r \times 1$ (where r is the number of parameters in the model), f is a nonlinear function of the predictor variables and the parameter vector, and ε_{ijk} is the within-group error including the within-group variance and correlation [26]; the error is assumed normally distributed with a mean of zero and a positive-definite variance-covariance structure R_{ij} , generally expressed as a function of the parameter vector δ [27].

$$\varepsilon_{ijk} \sim N(0, R_{ij}) \quad (1b)$$

Table 1. Summary statistics for both fitting and validation data.

Data	Variable	Min	Max	Mean	sd	Data	Variable	Min	Max	Mean	sd
Fitting data	QMD (cm)	10.2	23.2	17.4	3.69	Validation data	QMD (cm)	10.2	25.2	17.9	5.19
	MT(m)	5.0	21.3	16.0	3.13		MT (m)	5.0	21.3	15.9	3.88
	SD (tree ha ⁻¹)	800	4400	1905	849.68		SD (tree ha ⁻¹)	717	4400	1973	1168.08
	DD (cm)	10.1	25.7	21.8	3.28		DD (cm)	10.1	24.8	21.5	3.54
	DH (m)	7.3	30.3	21.6	4.12		DH (m)	7.3	26.3	20.4	3.91
	H (m)	7.1	27.7	18.3	4.82		H (m)	7.0	22.7	16.8	4.16
	BA (m ² ha ⁻¹)	15.67	68.00	37.24	14.12		BA (m ² ha ⁻¹)	15.67	59.43	37.72	13.19
	SA (m)	176	320	226	32.61		SA (m)	176	320	226	38.82
	SS (°)	15	41	29	6.32		SS (°)	23	41	32	3.50
	SI (m at 20 years)	12	24	20	2.83		SI (m at 20 years)	12	24	18	3.50
	SAG (yr)	5	37	24	6.98		SAG (yr)	6	38	26	8.79

QMD, plot quadratic mean diameter; MT, mean tree height of forest stand; SD, stand density; DD, plot dominant diameter; DH, plot dominant height; H, sample tree height; BA, basal area; SA, stand altitude; SS, stand slope; SI, site index; SAG, stand age; sd, standard deviation.
doi:10.1371/journal.pone.0104012.t001

Moreover, ϕ_{ij} can be expressed as:

$$\phi_{ij} = A_{ij}\lambda + B_{i,j}\mu_i + B_{ij}\mu_{ij} \tag{2a}$$

$$\mu_i \sim N(0, \psi_i), \mu_{ij} \sim N(0, \psi_{ij}) \tag{2b}$$

where λ is the $p \times 1$ vector of fixed population parameters (where p is the number of fixed parameters in the model). μ_i and μ_{ij} are the $q_1 \times 1$ and $q_2 \times 1$ vectors of random effects associated with the first and second levels, respectively (where q_1 and q_2 are the numbers of random parameters of two-level in the model), which are assumed to be normal (or Gaussian) with a mean of 0 and have the variance-covariance matrices ψ_i and ψ_{ij} ; these are the $q_1 \times q_1$ and $q_2 \times q_2$ variance-covariance matrices associated with the first and second level random effects, respectively. A_{ij} , $B_{i,j}$ and B_{ij} are the design matrices $r \times p$, $r \times q_1$ and $r \times q_2$ for the fixed and random effects specific to each sampling unit.

Individual-tree diameter growth equation. Five theoretical nonlinear growth equations, the Richards, Weibull, Korf, Logistic and Schumacher equations, were selected as candidates for modeling diameter growth. These equations are widely used for the simulation of individual-tree growth, particularly the Richards and Korf equations. Mathematical expressions of the equations are shown in Table 2.

The five above-mentioned equations are all S-shaped growth equations with inflection points and asymptotes. A characteristic of the Richards, Weibull and Korf equations is that the coordinates of the inflection points are variable multiples of asymptotic values; in contrast, the equivalent values of the logistic and Schumacher equations are fixed multiples [28]. The five equations were initially fit by *ONLS* regression using the R *nls* function without random parameters. Different initial values for the parameters were tried to ensure that a global minimum was achieved. The best performing function was selected as the base model by applying three statistical criteria; absolute mean residual (*AMR*), root mean square error (*RMSE*), and adjusted coefficient of determination (R^2_{adj}) [29]. The function with the smallest *AMR* and *RMSE* and the largest R^2_{adj} provides the best fit. The adjusted coefficient of determination is used similarly as an unbiased estimator in both multiple regression and canonical redundancy analysis. The formulas of the fit statistics are:

$$AMR = \sum_{i=1}^M \sum_{j=1}^{M_i} \sum_{k=1}^{n_{ij}} \frac{|y_{ijk} - \hat{y}_{ijk}|}{n_{ij}} \tag{3}$$

$$RMSE = \sqrt{\sum_{i=1}^M \sum_{j=1}^{M_i} \sum_{k=1}^{n_{ij}} \frac{(y_{ijk} - \hat{y}_{ijk})^2}{n_{ij} - r}} \tag{4}$$

$$R^2_{adj} = 1 - (n_{ij} - 1) \frac{\sum_{i=1}^M \sum_{j=1}^{M_i} \sum_{k=1}^{n_{ij}} \frac{(y_{ijk} - \hat{y}_{ijk})^2}{n_{ij} - r}}{\sum_{i=1}^M \sum_{j=1}^{M_i} \sum_{k=1}^{n_{ij}} (y_{ijk} - \bar{y})^2} \tag{5}$$

where \hat{y}_{ijk} is the predicted increment at the k th age within the j th tree within the i th plot. \bar{y} is the average of observations.

Table 2. Mathematical expressions of the five equations.

Equation	Expression	Inflection point		Parameters
		Abscissa	Ordinate	
Richards	$DBH = \phi_1(1 - \exp(-\phi_2 t))^{\phi_3}$	$1/(\phi_2 \ln \phi_3)$	$\phi_1(1 - 1/\phi_3)^{\phi_3}$	$\phi_1, \phi_2 > 0$
Weibull	$DBH = \phi_1(1 - \exp(-\phi_2 t^{\phi_3}))$	$((\phi_3 - 1)/\phi_2 \phi_3)^{1/\phi_3}$	$\phi_1(1 - \exp(1 - \phi_3)/\phi_3)$	$\phi_1, \phi_2, \phi_3 > 0$
Korf	$DBH = \phi_1 \exp(-\phi_2/t^{\phi_3})$	$((\phi_3 + 1)/\phi_2 \phi_3)^{-1/\phi_3}$	$\phi_1 \exp((\phi_3 - 1)/\phi_3)$	$\phi_1, \phi_2, \phi_3 > 0$
Logistic	$DBH = \phi_1/(1 + \exp(\phi_2 - \phi_3 t))$	ϕ_2/ϕ_3	$\phi_1/2$	$\phi_1, \phi_3 > 0$
Schumacher	$DBH = \phi_1 \exp(-\phi_2/t)$	$\phi_2/2$	$\phi_1 e^{-2}$	$\phi_1, \phi_2 > 0$

ϕ_1, ϕ_2 and ϕ_3 are the formal parameters.
doi:10.1371/journal.pone.0104012.t002

Mixed parameter evaluation. A crucial issue in fitting mixed-effects models is deciding which parameters should be considered random effects and which can be treated as fixed effects. A common approach is to start with random effects for all parameters and then to examine the fitted object to decide which, if any, of the random effects can be eliminated from the model [18]. Different combinations of model parameters were therefore tested to ascertain their contribution to predictions of diameter growth; the best model was selected by Akaike’s information criterion (AIC) [30], Bayesian information criterion (BIC) [31] and $-2 \log$ -likelihood ($-2 LL$) [32]. The best model gave the smallest AIC, BIC and $-2 LL$. The appropriate variance function and autoregressive structure for the NLME models were determined by the likelihood ratio test (LRT) [18,33]. All NLME models presented in this paper were calibrated using the *nlme* function in the R statistical environment [34].

Determining the variance-covariance structure. The variance-covariance matrices ψ_i and ψ_{ij} are positive-definite and symmetric, which is to say that all their eigenvalues must be strictly positive [18]. A hypothetical 2×2 variance-covariance matrix is shown as follows [24,35]:

$$\begin{bmatrix} \sigma_u^2 & \sigma_{uw} \\ \sigma_{wu} & \sigma_w^2 \end{bmatrix}$$

where σ_u^2 and σ_w^2 are the variance for the random effects u and w , respectively, and $\sigma_{uw} = \sigma_{wu}$ is the covariance between random effects u and w .

Determining the structure of R_{ij} . The matrix R_{ij} is allowed to depend on both random and fixed effects, as well as on a set of common but unknown parameters. The matrix accounts for within-plot heteroscedasticity and autocorrelation [24,26,27] by

including both correlation effects and weighting factors. The matrix is expressed as [24,36]:

$$R_{ij} = \sigma^2 G_{ij}^{0.5} I_{ij} G_{ij}^{0.5} \tag{6}$$

where for a tree j in plot i , with n_{ij} increment, R_{ij} is the $n_{ij} \times n_{ij}$ within-tree variance-covariance matrix that defines within-group variability, G_{ij} is an $n_{ij} \times n_{ij}$ diagonal matrix of within-tree error variance (heteroscedasticity), I_{ij} is an $n_{ij} \times n_{ij}$ matrix of within-tree autocorrelation of the errors, and σ^2 is a scaling factor for the error dispersion [13].

In individual-tree diameter growth models, the variance is often found dependent on the means, and the variance will generally increase with increasing mean tree diameter. To remove this effect, we modeled the variance as an exponential function or power function which was used for G_{ij} matrix [18]. And for the exponential function and power function, the diagonal elements of G_{ij} are $t_{ijk}^{2\delta}$ and $2\delta t_{ijk}$, respectively, and the off-diagonal elements are all 0.

$$\text{varexp}(\varepsilon_{ijk}) = \sigma^2 \exp(2\delta t_{ijk}) \tag{7}$$

$$\text{varpower}(\varepsilon_{ijk}) = \sigma^2 t_{ijk}^{2\delta} \tag{8}$$

Autocorrelation structures were used for I_{ij} matrix to address the within-tree autocorrelations of the errors observed in the data [37,38]. A method was selected from among three commonly used approaches: first-order autoregressive structure [AR(1)], a combination of first-order autoregressive and moving average structures [ARMA(1,1)], and the compound symmetry structure (CS) [18].

Table 3. Performance criteria for individual-tree diameter growth equations.

Equations	Fitting data			Validation data		
	AMR	RMSE	R^2_{adj}	AMR	RMSE	R^2_{adj}
Richards	2.2169	3.3224	0.7729	3.7228	4.7236	0.7448
Weibull	2.2724	3.3503	0.7690	3.7646	4.7196	0.7452
Korf	2.1286	3.2710	0.7855	3.6101	4.5369	0.7641
Logistic	2.3789	3.4523	0.7548	4.0064	5.0181	0.7120
Schumacher	2.1390	3.2808	0.7785	3.5979	4.6037	0.7576

doi:10.1371/journal.pone.0104012.t003

Table 4. Evaluation indices of each *NLME* model.

Effects	Mixed parameters	AIC	BIC	-2LL
Nested effects of plots and trees	ϕ_1	2992.3380	3022.0250	2980.3380
	ϕ_2	not converge		
	ϕ_3	3649.1130	3678.8010	3637.1140
	ϕ_1, ϕ_2	2164.7940	2214.2730	2144.7940
	ϕ_1, ϕ_3	2080.9480	2130.4270	2060.9480
	ϕ_2, ϕ_3	not converge		
	ϕ_1, ϕ_2, ϕ_3	not converge		
	Plots effects	ϕ_1	5151.7190	5176.4590
ϕ_2		5744.9100	5769.6500	5734.9100
ϕ_3		5209.6700	5234.4100	5199.6700
ϕ_1, ϕ_2		5146.6480	5181.2840	5132.6480
ϕ_1, ϕ_3		5145.6490	5180.2850	5131.6500
ϕ_2, ϕ_3		5168.1260	5202.7620	5154.1260
ϕ_1, ϕ_2, ϕ_3		not converge		
Trees effects	ϕ_1	2995.6300	3020.3690	2985.6300
	ϕ_2	4145.6660	4170.4060	4135.6660
	ϕ_3	3651.0750	3675.8150	3641.0760
	ϕ_1, ϕ_2	2167.8120	2202.4480	2153.8120
	ϕ_1, ϕ_3	2083.0270	2117.6630	2069.0280
	ϕ_2, ϕ_3	2102.0420	2151.5210	2082.0416
	ϕ_1, ϕ_2, ϕ_3	not converge		

doi:10.1371/journal.pone.0104012.t004

$$AR(1) = \sigma^2 \begin{bmatrix} 1 & \rho & \rho^2 \\ \rho & 1 & \rho \\ \rho^2 & \rho & 1 \end{bmatrix} \quad (9)$$

$$ARMA(1,1) = \sigma^2 \begin{bmatrix} 1 & \gamma & \gamma\rho \\ \gamma & 1 & \gamma \\ \gamma\rho & \gamma & 1 \end{bmatrix} \quad (10)$$

$$CS = \begin{bmatrix} \sigma^2 + \sigma_1 & \sigma_1 & \sigma_1 \\ \sigma_1 & \sigma^2 + \sigma_1 & \sigma_1 \\ \sigma_1 & \sigma_1 & \sigma^2 + \sigma_1 \end{bmatrix} \quad (11)$$

where ρ is the autoregressive parameter, γ is a moving average component, σ^2 is the residual variance, and σ_1 is the residual covariance [37–40].

Parameter estimation. The parameters in the equations were estimated by maximum likelihood (ML) using the Lindstrom and Bates (LB) algorithm implemented in the R *nlme* function [18,22]. The LB algorithm and *nlme* function are detailed in several articles (see, for example, [18,22]).

Predicting the random effects parameters is more problematic during model application and prediction than during the fitting process. In this case, they were estimated by the EBLUPs [25], using the increment data.

$$\hat{b}_i \approx \hat{D}\hat{Z}_i^T (\hat{R}_i + \hat{Z}_i\hat{D}\hat{Z}_i^T)^{-1} \hat{e}_i \quad (12)$$

where \hat{b}_i is the estimated random effects vector of EBLUPs, \hat{D} is the $q \times q$ estimated variance-covariance matrix (q is number of random-effects parameters) for the random effects, \hat{R}_i is the estimated variance-covariance matrix for the error term, \hat{Z}_i is the estimated partial derivatives matrix with respect to the random effects parameters for the new observation, and \hat{e}_i is the residual vector, whose dimension is the number of observations, and whose components are given by the difference between the observed diameter growth value for each tree, and the value predicted by the model including only fixed effects.

The standwise calibration was used to evaluate the accuracy of the calibration [12]. This type of calibration involves using the random plot components predicted from the increments of a small sample of trees per plot to predict the increment of the trees within the plot not used in the calibration. In this case, the calibration was made with 1, 2 and 3 trees per plot. The random parameters of new observations could be predicted with Equation 12.

Results

Function selection

The R *nls* function was used to evaluate the parameter estimates and model fit statistics of the five equations (Table 2); the results are listed in Table 3. The Korf equation had slightly better predictive ability than the others. Therefore, the Korf equation was selected as the basic nonlinear model for estimating diameter growth. The final base model is given by:

Table 5. Performance criteria for the best NLME models.

Effects	Mixed parameters	AIC	BIC	-2LL	LRT	p Value
Plots effects	ϕ_1	5151.72	5176.46	5141.72		
	ϕ_1, ϕ_3	5145.65	5180.29	5131.65	10.07	0.0065
	ϕ_1, ϕ_3 with exponential function and ARMA(1,1)	2042.40	2091.88	2022.40	3109.24	<0.0001
Trees effects	ϕ_1	2995.63	3020.37	2985.63		
	ϕ_1, ϕ_3	2083.03	2117.66	2069.03	916.60	<0.0001
	ϕ_1, ϕ_3 with exponential function and ARMA(1,1)	1113.96	1163.44	1093.96	975.07	<0.0001
Nested effects of plots and trees	ϕ_1	2992.34	3022.03	2980.34		
	ϕ_1, ϕ_3	2080.95	2130.43	2060.95	919.39	<0.0001
	ϕ_1, ϕ_3 with exponential function and ARMA(1,1)	1112.75	1177.07	1086.75	974.20	<0.0001

doi:10.1371/journal.pone.0104012.t005

$$DBH_{ijk} = \phi_1 \exp\left(-\phi_2 / t_{ijk}^{\phi_3}\right) + \varepsilon_{ijk} \quad (13)$$

NLME model construction

The approach used to construct the NLME models was to fit the models with nested effects of plot and tree for Equation 13 and then to successively remove the random effects. The results are listed in Table 4. Four of the NLME models reached convergence with nested effects of plot and tree; the fifth and sixth models converged when the one-level models included the random effects of plot and tree, respectively.

LRT, AIC, BIC and -2 LL fit statistics were compared among different combinations of random effects parameters (Table 4). The models represented by Equations 14–16, incorporating the nested effects of plot and tree, plot effects and tree effects on ϕ_1 and ϕ_3 , yielded the smallest AIC, BIC and -2 LL.

$$DBH_{ijk}^{p \text{ and } t} = (\beta_1 + u_{1i} + u_{1ij}) \exp\left(-\beta_2 / t_{ijk}^{(\beta_3 + u_{3i} + u_{3ij})}\right) + \varepsilon_{ijk} \quad (14)$$

$$DBH_{ijk}^p = (\beta_1 + u_{1i}) \exp\left(-\beta_2 / t_{ijk}^{(\beta_3 + u_{3i})}\right) + \varepsilon_{ijk} \quad (15)$$

$$DBH_{ijk}^t = (\beta_1 + u_{1j}) \exp\left(-\beta_2 / t_{ijk}^{(\beta_3 + u_{3j})}\right) + \varepsilon_{ijk} \quad (16)$$

where $DBH_{ijk}^{p \text{ and } t}$ and DBH_{ijk}^p , DBH_{ijk}^t are the diameters at breast height for the three effects; β_1 , β_2 and β_3 are fixed-effects parameters; u_{1i} and u_{3i} are random-effects parameters generated by plot on ϕ_1 and ϕ_3 , respectively; u_{1j} and u_{3j} are random-effects parameters generated by tree on ϕ_1 and ϕ_3 , respectively; and u_{1ij} and u_{3ij} are random-effects parameters generated by interaction of plot and tree on ϕ_1 and ϕ_3 , respectively.

NLME models with heteroscedasticity and autocorrelation

We used the power function or the exponential function as the variance functions and the AR(1), ARMA(1,1) or CS as the autocorrelation structures to fit diameter growth models incorporating different random effects. The results of the models provided the best fit are shown in Table 5. The selected models had the smallest AIC, BIC and -2 LL. Thus, the final models of plot effects, tree effects and the two nested effects are, respectively:

$$\text{Equation 14 + Equation 7 + Equation 10} \quad (17)$$

$$\text{Equation 15 + Equation 8 + Equation 10} \quad (18)$$

$$\text{Equation 16 + Equation 7 + Equation 10} \quad (19)$$

Parameter estimates

Nested effects of plot and tree. The nested two-level NLME diameter growth model is:

$$DBH_{ijk}^{p \text{ and } t} = (27.2796 + u_{1i} + u_{1ij}) \exp\left(-24.7556 / t_{ijk}^{(1.5416 + u_{3i} + u_{3ij})}\right) + \varepsilon_{ijk} \quad (20a)$$

where

$$\mu_i = \begin{bmatrix} u_{1i} \\ u_{3i} \end{bmatrix} \sim N\left\{\begin{bmatrix} 0 \\ 0 \end{bmatrix}, \psi_i = \begin{pmatrix} 3.5713 & -0.1411 \\ -0.1411 & 0.0640 \end{pmatrix}\right\} \quad (20b)$$

$$\mu_{ij} = \begin{bmatrix} u_{1ij} \\ u_{3ij} \end{bmatrix} \sim N\left\{\begin{bmatrix} 0 \\ 0 \end{bmatrix}, \psi_{ij} = \begin{pmatrix} 6.0658 & -0.5052 \\ -0.5052 & 0.0788 \end{pmatrix}\right\} \quad (20c)$$

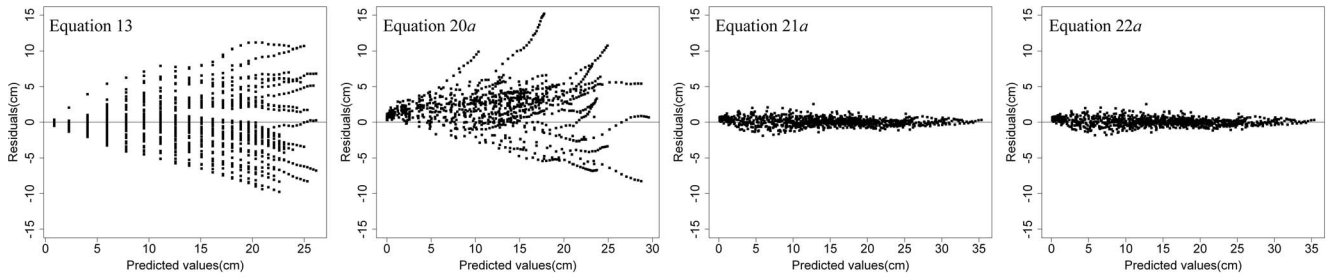


Figure 2. Residual error map of diameter growth of each model.
doi:10.1371/journal.pone.0104012.g002

$$\varepsilon_{ijk} \sim N\left(0, R_{ijk} = 1.0700 G_{ij}^{0.5} I_{ij} G_{ij}^{0.5}\right) \quad (20d)$$

$$\text{var exp}(\varepsilon_{ijk}) = 1.0700 \exp(-0.0724 t_{ijk}) \quad (20e)$$

$$\text{ARMA}(1,1) = 1.0700 \times \begin{bmatrix} 1 & 0.7842 & 0.2456 \\ 0.7842 & 1 & 0.7842 \\ 0.2456 & 0.7842 & 1 \end{bmatrix} \quad (20f)$$

Plot effects. The NLME diameter growth model incorporating the effect of plot is:

$$\text{DBH}_{ijk}^p = (21.9361 + u_{1i}) \exp\left(-52.3880 / t_{ijk}^{(1.9153 + u_{3i})}\right) + \varepsilon_{ijk} \quad (21a)$$

where

$$\mu_i = \begin{bmatrix} u_{1i} \\ u_{3i} \end{bmatrix} \sim N\left\{\begin{bmatrix} 0 \\ 0 \end{bmatrix}, \psi_i = \begin{pmatrix} 5.2409 & -0.2937 \\ -0.2937 & 0.0910 \end{pmatrix}\right\} \quad (21b)$$

$$\varepsilon_{ijk} \sim N\left(0, R_{ijk} = 2.3484 G_{ij}^{0.5} I_{ij} G_{ij}^{0.5}\right) \quad (21c)$$

$$\text{var power}(\varepsilon_{ijk}) = 2.3484 t_{ijk}^{0.4498} \quad (21d)$$

$$\text{ARMA}(1,1) = 2.3484 \times \begin{bmatrix} 1 & 0.9822 & 0.1811 \\ 0.9822 & 1 & 0.9822 \\ 0.1811 & 0.9822 & 1 \end{bmatrix} \quad (21e)$$

Tree effects. The NLME diameter growth model incorporating the effect of tree is:

$$\text{DBH}_{ijk}^t = (27.2695 + u_{1j}) \exp\left(-24.6702 / t_{ijk}^{(1.5367 + u_{3j})}\right) + \varepsilon_{ijk} \quad (22a)$$

where

$$\mu_j = \begin{bmatrix} u_{1j} \\ u_{3j} \end{bmatrix} \sim N\left\{\begin{bmatrix} 0 \\ 0 \end{bmatrix}, \psi_j = \begin{pmatrix} 7.1218 & -0.4005 \\ -0.4005 & 0.0983 \end{pmatrix}\right\} \quad (22b)$$

$$\varepsilon_{ijk} \sim N\left(0, R_{ijk} = 1.0729 G_{ij}^{0.5} I_{ij} G_{ij}^{0.5}\right) \quad (22c)$$

$$\text{var exp}(\varepsilon_{ijk}) = 1.0729 \exp(-0.0727 t_{ijk}) \quad (22d)$$

$$\text{ARMA}(1,1) = 1.0729 \times \begin{bmatrix} 1 & 0.7852 & 0.2455 \\ 0.7852 & 1 & 0.7852 \\ 0.2455 & 0.7852 & 1 \end{bmatrix} \quad (22e)$$

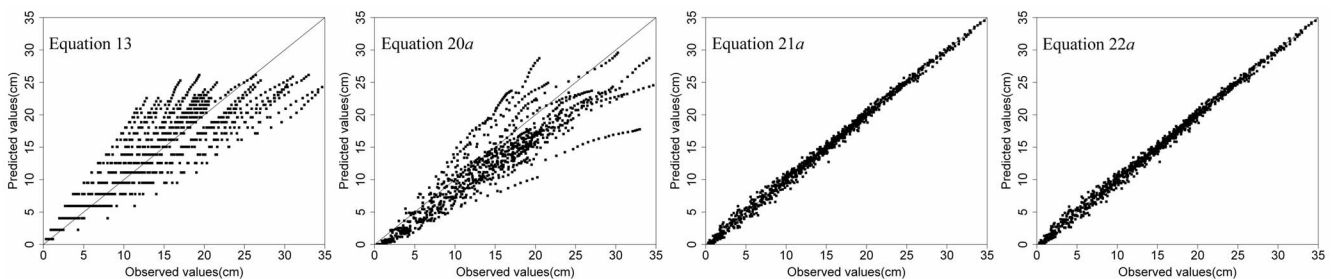


Figure 3. Scatter plot of fitted values against observed values of diameter growth of each model.
doi:10.1371/journal.pone.0104012.g003

Table 6. Performance criteria of each model.

Equation	Effect	Fitting data			Validation data		
		AMR	RMSE	R^2_{adj}	AMR	RMSE	R^2_{adj}
Equation 13		2.1286	3.2810	0.7785	3.6101	4.6369	0.7541
Equation 20a	Fixed effects	3.1584	2.4843	0.7251	4.0866	5.7676	0.6217
	Mixed effects	2.1722	3.6806	0.7929	2.9457	4.6317	0.7560
Equation 21a	Fixed effects	2.9172	2.0876	0.8059	3.8138	4.9368	0.7228
	Mixed effects	0.4027	0.5350	0.9956	0.6816	2.0699	0.9513
Equation 22a	Fixed effects	2.9170	2.0875	0.8059	3.8204	4.9357	0.7229
	Mixed effects	0.4025	0.5344	0.9957	0.6804	1.8842	0.9596

doi:10.1371/journal.pone.0104012.t006

Model prediction

The predictive ability of Equation 13 was evaluated using predict procedures and Equations 3–5 on both fitting and validation data. The performance of the *NLME* models, with and without modeling the error structure, was evaluated using cross-validation procedures for both fitting and validation data; the random effects were predicted with the EBLUPs (Equation 12), using the measurement data.

Table 6 lists the three fit statistics for Equation 13 and Equations 20a–22a with and without random effects. Equation 20a was the best predictor, with increases in R^2_{adj} and decreases in *AMR* and *RMSE* for both fitting and validation data, but it was more complex than the others and incurred significant computing cost. In Figure 2, the residuals of Equations 13 and 20a–22a are plotted against the fitted values; the fitted values are plotted against the observed values in Figure 3. Based on the above analysis, we can conclude that, although Equation 20a is the strongest predictor, it is more complex than Equation 22a and the difference between them is small. Compared with Equation 13, Equation 22a had a higher R^2_{adj} , 0.9956 compared to 0.7758, and a lower *RMSE*, 0.5344 compared to 3.2810. Therefore, the *NLME* model incorporating the random effect of trees was the best model for predicting diameter growth of individual China-fir trees in the single-species plantations of the study area.

Discussion

Of the 5 theoretical growth equations tested, the Korf equation best fit the individual-tree diameter growth data of China-fir when evaluated on the basis of *AMR*, *RMSE* and R^2_{adj} . The Korf equation is widely used for forest growth and yield simulation models [41–43]. *ONLS* regression is commonly used to build forest growth models, but its value is limited because tree data typically violate the assumption of independent and identically distributed errors [13,44,45]. *NLME* models are a useful tool for analyzing repeated measures data and spatially correlated data [18,33]. A model can be constructed with a unique variance-covariance structure that eliminates the influence of the random effects (plot and tree effects in this study). The two primary challenges in fitting *NLME* models are determining the mixed parameters and calculating the random effects [9,18,24,33,46]. An additional source of inherent correlation would be the effect of year, where observations coming from the same year would be highly correlated; tree-ring width is largely related with yearly climate variables [47]. However, year effects were not analyzed in this study. Incorporating annual climate factors into the *NLME* models may be an appropriate area for future research.

The Korf equation has been widely used as the base *NLME* model for forest growth and yield prediction. For example, Cheng and Gordon [48] successfully used the Korf equation with *NLME* models to fit loblolly pine (*Pinus taeda* L.) diameter-age relationships; the one-level (tree) individual-tree *NLME* model, based on the Korf equation, with random effects parameters ϕ_1 and ϕ_3 had the best fit. Parameters ϕ_1 , ϕ_2 and ϕ_3 are the asymptotic values, the values associated with the growth rate of the tree and the values associated with the curve shape (inflection point) of the Korf equation, respectively. Therefore, the random effects (tree) mainly influence the maximum value and the inflection point, with evidence that the growth rate of the tree affects the model fit.

Sometimes, no prior information is available from which the random parameters can be predicted. In this case, the mixed-effects model with the random parameters set to 0 is not the same

as the population average model and will give biased predictions. Instead, the population average model, fit without random effects, should be used.

Conclusions

Five theoretical growth equations were evaluated for estimating the diameter growth of China-fir trees grown in monospecific plantations in Fujian province, southeast China. The equations can be evaluated for both biological and statistical meaning. All 5 equations and the Korf equation in particular were commonly and successfully used to model individual-tree diameter growth. One-level (plot or tree) and nested two-level (tree nested within plot) NLME models based on the Korf equation, with variance functions and correlation structures, were used to estimate diameter growth of individual trees; this approach was necessitated by the hierarchical structure of the experimental design and the

autocorrelated tree-ring data. The results showed that the one-level (tree) NLME model (Equation 22a) with random effects was better than the others (Equations 13, 20a and 21a) (Table 5, Figure 2 and 3). Therefore, we recommend using nonlinear mixed-effects models to estimate individual-tree diameter growth.

Acknowledgments

The authors thank teachers Jinghui Meng, Lushuang Gao, Jin Wang, Jing Fang and other researchers in major of Forest Management in Beijing Forestry University for this study.

Author Contributions

Conceived and designed the experiments: HX YS XW. Performed the experiments: HX YF YD YL. Analyzed the data: HX YF YD YL. Contributed reagents/materials/analysis tools: HX YS YF YD. Wrote the manuscript: HX. Revised the manuscript: YS XW.

References

- Leites LP, Robinson AP, Crookston NL (2009) Accuracy and equivalence testing of crown ratio models and assessment of their impact on diameter growth and basal area increment predictions of two variants of the Forest Vegetation Simulator. *Can J Forest Res* 3: 655–665.
- Vanclay JK (1994) Modelling forest growth and yield: applications to mixed tropical forests. School of Environmental Science and Management Papers 537.
- Adame P, Hynynen J, Canellas I, Del Rio M (2008) Individual-tree diameter growth model for rebollo oak (*Quercus pyrenaica* Willd.) coppices. *Forest Ecol Manag* 3–4: 1011–1022.
- Lhotka JM, Loewenstein EF (2011) An individual-tree diameter growth model for managed uneven-aged oak-shortleaf pine stands in the Ozark Highlands of Missouri, USA. *Forest Ecol Manag* 3: 770–778.
- Timilsina N, Staudhammer CL (2013) Individual Tree-Based Diameter Growth Model of Slash Pine in Florida Using Nonlinear Mixed Modeling. *Forest Sci* 1: 27–37.
- Wykoff WR (1990) A basal area increment model for individual conifers in the northern Rocky Mountains. *Forest Sci* 4: 1077–1104.
- Port E A, Bartelink HH (2002) Modelling mixed forest growth: a review of models for forest management. *Ecol Model* 1: 141–188.
- Grégoire TG, Schabenberger O, Barrett JP (1995) Linear modelling of irregularly spaced, unbalanced, longitudinal data from permanent-plot measurements. *Canadian Journal of Forest Research* 25: 137–156.
- Uzoh FCC, Oliver WW (2008) Individual tree diameter increment model for managed even-aged stands of ponderosa pine throughout the western United States using a multilevel linear mixed effects model. *Forest Ecol Manag* 3: 438–445.
- Fox JC, Ades PK, Bi H (2001) Stochastic structure and individual-tree growth models. *Forest Ecol Manag* 1: 261–276.
- Biging GS (1985) Improved estimates of site index curves using a varying-parameter mode. *Forest Sci* 1: 248–259.
- Calama R, Montero G (2005) Multilevel linear mixed model for tree diameter increment in stone pine (*Pinus pinea*): a calibrating approach. *Silva Fenn* 1: 37–54.
- Gregoire TG (1995) Linear modelling of irregularly spaced, unbalanced, longitudinal data from permanent-plot measurements. *Can J Forest Res* 25: 137–156.
- Keselman HJ, Algina J, Kowalchuk RK, Wolfinger RD (1999) A comparison of recent approaches to the analysis of repeated measurements. *British Journal of Mathematical and Statistical Psychology* 52: 63–78.
- Lappi J (1986) Mixed linear models for analyzing and predicting stem form variation of Scots pine. Helsinki: Finnish Forest Research Institute. 354 p.
- Schabenberger O, Gregoire TG (1995) A conspectus on estimating function theory and its application to recurrent modelling issues in forest biometry. *Silva Fenn* 1: 49–70.
- Rathbun LC, Lemay V, Smith N (2011) Diameter growth models for mixed-species stands of Coastal British Columbia including thinning and fertilization effects. *Ecol Model* 145: 2234–2248.
- Pinheiro JC, Bates DM (2000) *Mixed Effects Models in S and S-Plus*. New York:Spring-Verlag. 534 p.
- Nigh G (2012) Calculating empirical best linear unbiased predictors (EBLUPs) for nonlinear mixed effects models in Excel/Solver. *Forest Chron* 3: 340–344.
- Wolfinger RD (1999) Fitting nonlinear mixed models with the new NLMIXED procedure
- Pinheiro JC, Bates DM (1995) Model building for nonlinear mixed effects models. *Citeseer*. 256 p.
- Lindstrom MJ, Bates DM (1990) Nonlinear mixed effects models for repeated measures data. *Biometrics* 673–687.
- Palmer MJ, Phillips BF, Smith GT (1991) Application of nonlinear models with random coefficients to growth data. *Biometrics* 623–635.
- Calama R, Montero G (2004) Interregional nonlinear height-diameter model with random coefficients for stone pine in Spain. *Can J Forest Res* 1: 150–163.
- Vonesh E, Chinchilli VM (1997) *Linear and Nonlinear Models for the Analysis of Repeated Measurements*. New York:Marcel Dekker. 495 p.
- Davidian M, Giltinan DM (1995) *Nonlinear Models for Repeated Measurement Data*. New York: Chapman & Hall. 451 p.
- Meng SX, Huang S (2009) Improved calibration of nonlinear mixed-effects models demonstrated on a height growth function. *Forest Sci* 3: 238–248.
- Anta MB, Dorado FC, Di E Guez-Aranda U, Alvarez Gonzalez JG, Parresol BR, et al (2006) Development of a basal area growth system for maritime pine in northwestern Spain using the generalized algebraic difference approach. *Canadian journal of forest research* 6: 1461–1474.
- Zhang JG, Duan AG, Sun HG, Fu LH (2011) Self-thinning and growth modelling for even-aged Chinese fir (*Cunninghamia lanceolata* (Lamb.) Hook.) stands. Beijing: Science Press. 381 p.
- Akaike H (1974) A new look at the statistical model identification. *Automatic Control, IEEE Transactions on* 6: 716–723.
- Weiss RE (2005) *Modeling longitudinal data*. New York: Springer. 572 p.
- Zhao L, Li C, Tang S (2012) Individual-tree diameter growth model for fir plantations based on multi-level linear mixed effects models across southeast China. *Journal of Forest Research* 4: 305–315.
- Fang Z, Bailey RL (2001) Nonlinear mixed effects modeling for slash pine dominant height growth following intensive silvicultural treatments. *Forest Sci* 3: 287–300.
- Ihaka R, Gentleman R (2004) R: a language and environment for statistical computing Vienna, Austria: R Foundation for Statistical Computing.
- Fu L, Sun H, Sharma RP, Lei Y, Zhang H, et al (2013) Nonlinear mixed-effects crown width models for individual trees of Chinese fir (*Cunninghamia lanceolata*) in south-central China. *Forest Ecol Manag* 210–220.
- Crecente-Campo F, Soares P, Tome M, Dieguez-Aranda U (2010) Modelling annual individual-tree growth and mortality of Scots pine with data obtained at irregular measurement intervals and containing missing observations. *Forest Ecol Manag* 11: 1965–1974.
- Lappi J, Malinen J (1994) Random parameter height-age models when stand parameters and stand age are correlated. *Forest Sci* 4: 715–731.
- Omule SAY, MacDonald RN (1991) Simultaneous curve fitting for repeated height-diameter measurements. *Can J Forest Res* 9: 1418–1422.
- Gregorie TG (1987) Generalized error structure for forestry yield models. *Forest Sci* 2: 423–444.
- Leak W (1996) Analysis of multiple systematic remeasurement. *Forest Sci* 12: 69–73.
- Castedo-Dorado F, Dieguez-Aranda U, Barrio-Anta M, Alvarez-Gonzalez JG (2007) Modelling stand basal area growth for radiata pine plantations in Northwestern Spain using the GADA. *Ann Forest Sci* 6: 609–619.
- Fontes L, Tome M, Coelho MB, Wright H, Luis JS, et al (2003) Modelling dominant height growth of Douglas-fir (*Pseudotsuga menziesii* (Mirb.) Franco) in Portugal. *Forestry* 5: 509–523.
- Kitikidou K, Petrou P, Milios E (2012) Dominant height growth and site index curves for Calabrian pine (*Pinus brutia* Ten.) in central Cyprus. *Renew Sust Energ Rev* 2: 1323–1329.
- Jordon L, Daniels RF, Clark A, He R (2005) Multilevel nonlinear mixed-effects models for the modeling of earlywood and latewood microfibril angle. *Forest Sci* 4: 357–371.
- West PW, Ratkowsky DA, Davis AW (1984) Problems of hypothesis testing of regressions with multiple measurements from individual sampling units. *Forest Ecol Manag* 3: 207–224.
- Yang YQ, Huang SM, Trincado G, Meng SX (2009) Nonlinear mixed-effects modeling of variable-exponent taper equations for lodgepole pine in Alberta, Canada. *European Journal of Forest Research* 4: 415–429.

47. Laubhann D, Sterba H, Reinds GJ, De Vries W (2009) The impact of atmospheric deposition and climate on forest growth in European monitoring plots: An individual tree growth model. *Forest Ecol Manag* 8: 1751–1761.
48. Cheng C, Gordon DN (2012) An analysis and comparison of predictors of random parameters demonstrated on planted loblolly pine diameter growth prediction. *Forestry* 2: 271–280.